THE JOURNAL OF PHYSICAL CHEMISTRY C

Article

Single-Crystalline and Twinned ZnP Nanowires: Synthesis, Characterization, and Electronic Properties

Guozhen Shen, Po-Chiang Chen, Yoshio Bando, Dmitri Golberg, and Chongwu Zhou

J. Phys. Chem. C, **2008**, 112 (42), 16405-16410• DOI: 10.1021/jp806334k • Publication Date (Web): 27 September 2008

Single-Crystalline and Twinned Zn_3P_2 Nanowires: Synthesis, Characterization, and Electronic Properties

Guozhen Shen,*,† Po-Chiang Chen,† Yoshio Bando,‡ Dmitri Golberg,‡ and Chongwu Zhou†

Department of Electrical Engineering, University of Southern California, Los Angeles, California 90089, and Nanoscale Materials Center and World Premier International Center for Materials Nanoarchitectonics (MANA), National Institute for Materials Science (NIMS), Namiki 1-1, Tsukuba, Ibaraki 305-0044, Japan

Received: July 18, 2008; Revised Manuscript Received: August 24, 2008

We describe the synthesis of zigzag-shaped single-crystalline or twinned Zn_3P_2 nanowires via a thermochemical method. The single-crystalline nanowires possessed two different kinds of kink angles and were formed via a vapor−solid process by using ZnS and GaP as source materials, whereas the twinned nanowires were synthesized via a vapor−liquid−solid process under additional introduction of In_2S_3 nanoparticles as the catalyst precursors. The products were characterized in detail by using X-ray diffraction, a scanning electron microscope, and a transmission electron microscope equipped with an energy-dispersive X-ray spectrometer. Field-effect transistors based on individual zigzag nanowires were fabricated and their electronic transport at different temperatures was analyzed. The results showed that these unusual structures are p-type semiconductors and that the thermal activation with a 49.7 meV energy is the dominant transport mechanism.

1. Introduction

As one of the II−V group semiconductors, bulk and thin films of Zn_3P_2 have actively been studied for photovoltaic applications.[1−3] Zn_3P_2 has a direct band gap of 1.5 eV, which is the optimum range for photovoltaic solar energy conversion. Energy conversion efficiency of 5.96% was found on polycrystalline transparent magnesium Zn_3P_2 diodes.[1] Both of the Zn_3P_2 constituent elements, Zn and P, are abundant in nature and cheap, which makes it possible for the deployment of low-cost solar cells. Besides, Zn_3P_2 has promising applications in developing Li-ion batteries because of its low polarization, as well as decent potentials of reactions with Li during initial and successive cycles. Li can be inserted into Zn_3P_2 via two distinct pathways, forming LiZnP, Li_4ZnP_2, Li_3P, $LiZn_4$, LiZn, etc. with a large number of inserted Li atoms (up to 6).[4,5] It is thought that one-dimensional (1-D) nanomaterials have well-defined domain structures with clearly identifiable grain boundaries, thus the fabrication of 1-D Zn_3P_2 nanostructures provides better possibilities for the investigation of the Li−Zn_3P_2 interactions. However, such promise cannot be accomplished without establishing a general method for synthesizing required 1-D Zn_3P_2 nanostructures on a large scale. Until now, only a few reports could be found on the synthesis of 1-D Zn_3P_2 nanomaterials[6−10] and only one report on electrical studies of Zn_3P_2 nanobelts has become available.[9] Thus it is still a great challenge to synthesize other 1-D Zn_3P_2 nanostructures with special morphologies and to study their electronic properties.

In this paper, we report on the synthesis of zigzag-shaped Zn_3P_2 nanowires on a large scale via a simple thermochemical method. Governed by different growth mechanisms, both single-crystalline and twinned zigzag Zn_3P_2 nanowires have been obtained on a large scale. In addition, novel field-effect transistors (FETs) based on individual Zn_3P_2 nanowires have been constructed and their low-temperature electron transport was investigated.

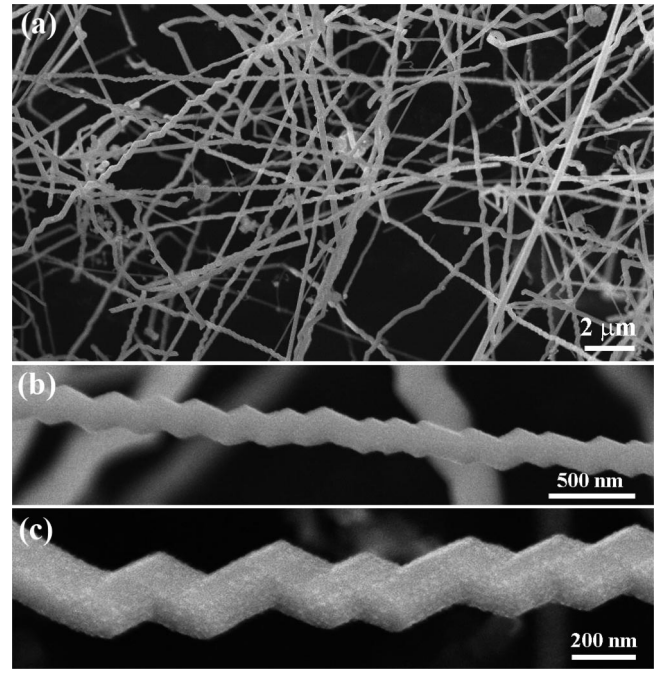

Figure 1. SEM images of zigzag Zn_3P_2 nanowires at different magnifications.

2. Experimental Section

Zigzag-shaped Zn_3P_2 nanowires were synthesized in a vertical high-frequency induction furnace. The furnace consists of a fused quartz tube and an induction-heated cylinder made of high-purity graphite coated with a carbon fiber thermoinsulating layer and has one inlet and one outlet on its base.[6,8] In a typical process, a graphite crucible, containing a mixture of ZnS and GaP at a molar ratio of 1:1.3, was placed at the center cylinder

* Author to whom correspondence should be addressed. E-mail: guozhens@usc.edu.
† University of Southern California.
‡ Nanoscale Materials Center and World Premier International Center for Materials Nanoarchitectonics.

10.1021/jp806334k CCC: $40.75
Published on Web 09/27/2008

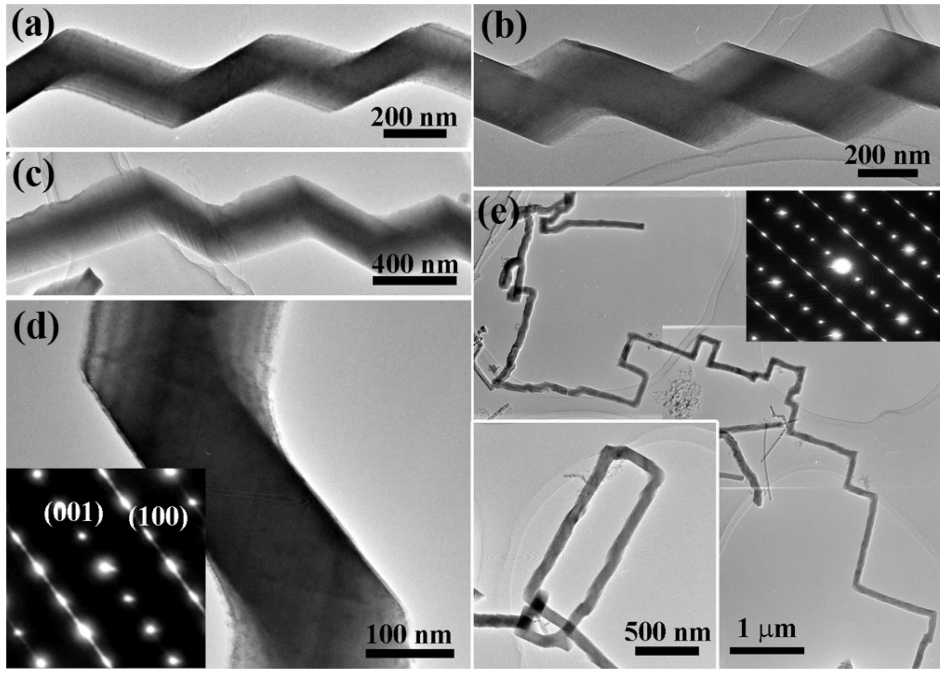

Figure 2. (a−c) TEM images of typical zigzag Zn_3P_2 nanowires, showing angles of 120° between two neighboring kinks. (d) TEM image of a single kink and its corresponding SAED pattern. (e) TEM image of another kind of zigzag Zn_3P_2 nanowires with angles of 90° between two neighboring kinks. Insets: SAED pattern of a nanowire (upper) and TEM image of a highly curved square ring-like Zn_3P_2 nanowire (bottom).

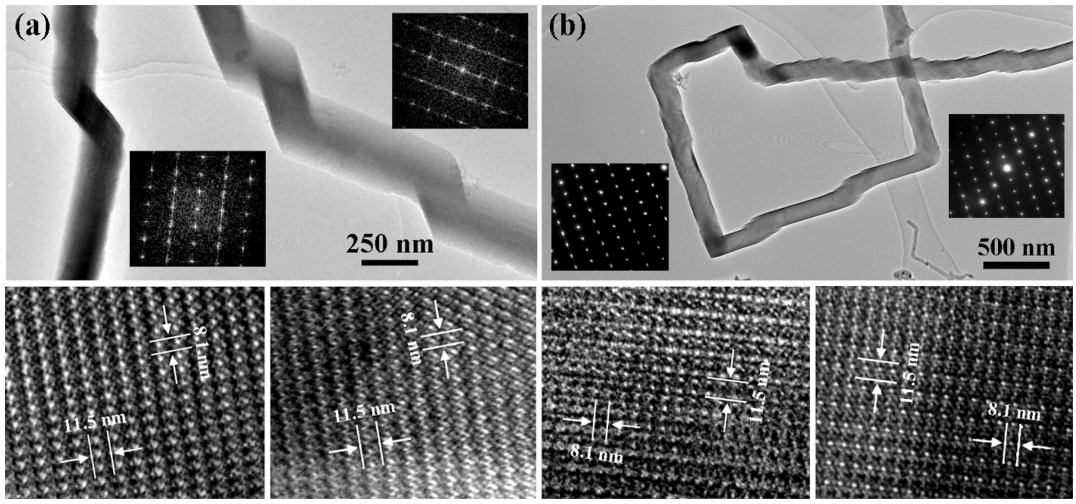

Figure 3. (a) Zigzag Zn_3P_2 nanowires with 120° angles between two neighboring kinks. (b) Zigzag Zn_3P_2 nanowires with 90° angles between kinks. The insets in the bottom are HRTEM images and the upper frames illustrate the diffraction patterns.

zone. After evacuation of the quartz tube to ~20 Pa, an Ar flow was introduced into the system through the inlet at a flow rate of 150 sccm. After flowing for 30 min, the crucible was rapidly heated to 1400 °C within 10 min and maintained at this temperature for 1 h under ambient pressure. After the crucible was cooled to room temperature, a yellowish wool-like product was found deposited on the inner wall of the graphite cylinder. During the reaction, the processing temperature was measured by an optical pyrometer with an estimated accuracy of ±10 °C. To get twinned zigzag Zn_3P_2 nanowires, extra In_2S_3 nanoparticles were mixed with ZnS and GaP as the source materials while other conditions were kept unchanged.

The structures and morphologies of the products were characterized by using an X-ray powder diffractometer (RINT 2200F) with Cu Kα radiation, a scanning electron microscope (SEM, JSM-6700F), and a field-emission transmission electron microscope (TEM, JEM-3000F) equipped with an energy-dispersive X-ray spectrometer (EDS).

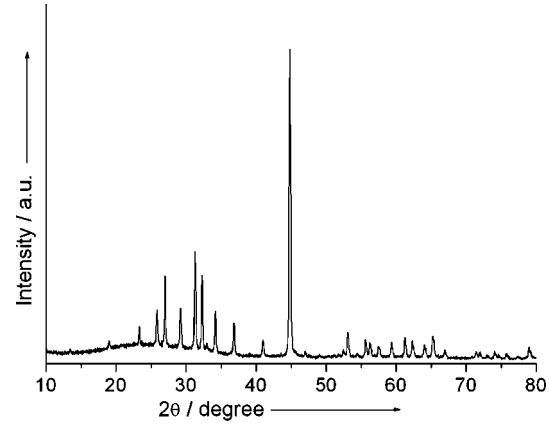

Figure 4. XRD pattern of the twinned zigzag Zn_3P_2 nanowires.

Single-nanowire-based FETs were then fabricated according to a technique reported by us previously.[11−13] Briefly, the zigzag

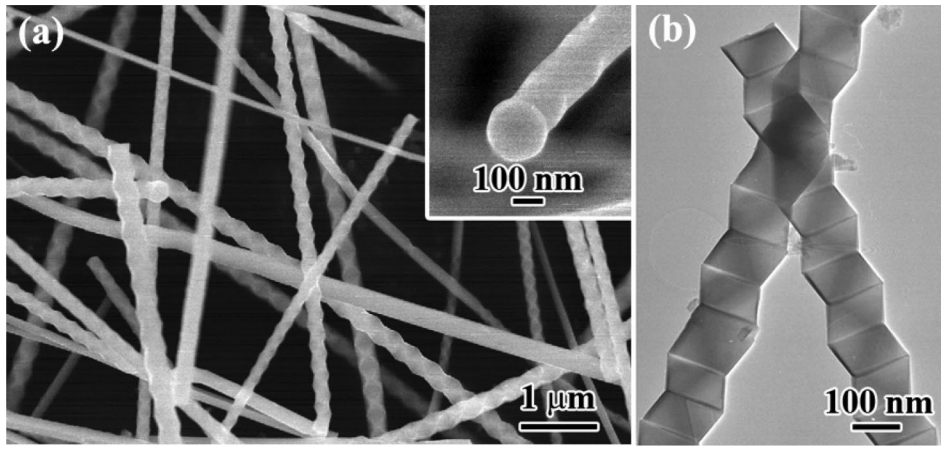

Figure 5. (a) SEM image and (b) TEM image of the twinned zigzag Zn_3P_2 nanowires. Inset: SEM image of the tip of a nanowire, showing the attached nanoparticles.

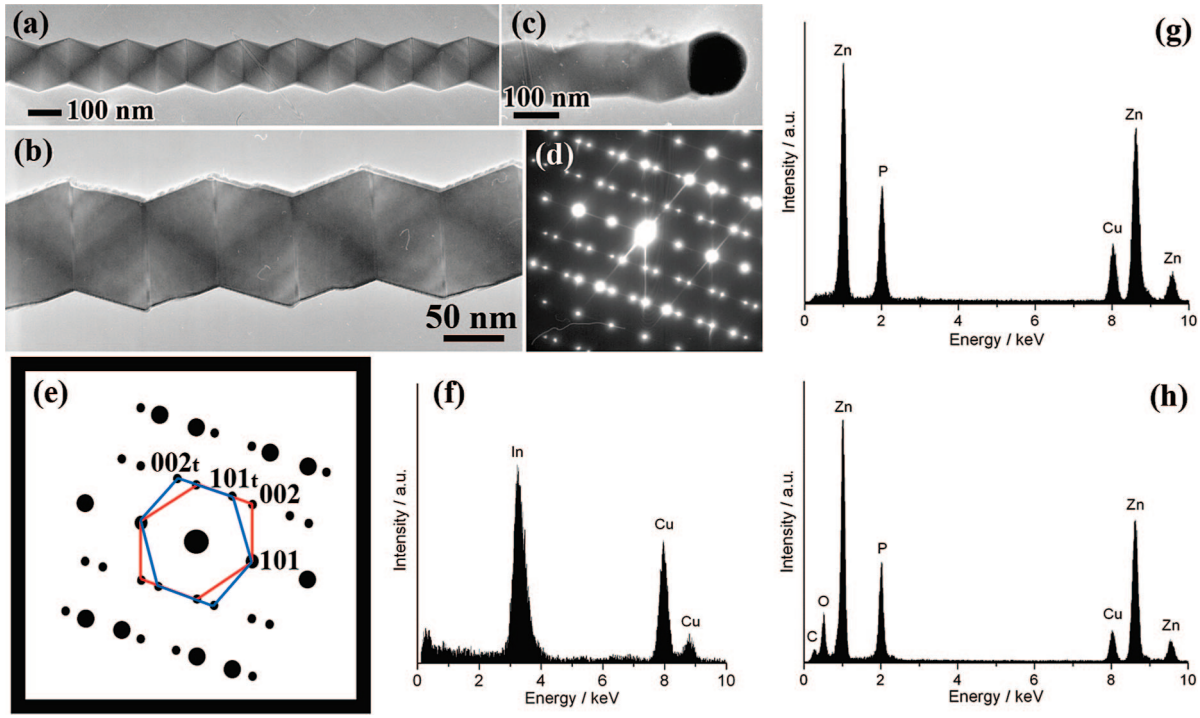

Figure 6. TEM image of (a, b) a twinned zigzag Zn_3P_2 nanowire, (c) its tip, and (d, e) the corresponding SAED pattern (f−h). EDS spectra are taken from the attached particle, the nanowire body, and its surface, respectively.

Zn_3P_2 nanowires were first sonicated into a suspension in isopropanol and then deposited onto a degenerately doped silicon wafer covered with a 500 nm SiO_2 layer. Photolithography was then performed, followed by the Ti/Au deposition to pattern the source and drain electrodes on both ends of the nanowires.

3. Results and Discussion

3.1. Single-Crystalline Zigzag Zn_3P_2 Nanowires. After reaction, the product was directly checked by using XRD and the result reveals the formation of a pure tetragonal Zn_3P_2 phase (JCPDS No. 65-2854). Figure 1a shows a typical SEM image of the as-grown nanowires. Most of the nanowires are of zigzag shapes, contrary to straight Zn_3P_2 nanowires reported before.[8,9] The nanowire diameters range from 70 to 300 nm and lengths reach up to over 100 μm. No particles were found attached to the tips, indicating the vapor−solid (VS) growth mechanism. High-magnification SEM images of typical zigzag Zn_3P_2 nanowires are shown in Figure 1, panels b and c. The zigzag nanowires are of uncommon rectangle-like cross sections, not the round ones observed for many nanowires.[14−20]

To characterize the chemical compositions and structures, we carried out TEM, EDS, and selected-area electron diffraction (SAED) studies. Panels a−c of Figures 2 depict TEM images of three periods in three typical zigzag Zn_3P_2 nanowires, which have diameters of 170, 200, and 300 nm, respectively. The periodicity along the wires is 400, 400, and 700 nm long, and 300, 350, 400 nm wide, respectively. For all kinds of nanowires, the angle between the two neighboring kinks is ∼120°, which is consistent with that between the (001) and (101) planes. A higher magnification TEM image of a single kink is shown in Figure 2d. Its SAED pattern is displayed in the inset. This reveals that the nanowire is a single crystal. Diffraction patterns of various kinks reveal exactly the same appearance without the need to tilt the sample, which indicates the uniformity of a crystalline state. Besides the mentioned kind of zigzag Zn_3P_2 nanowires, another kind with a 90° angle between the two close

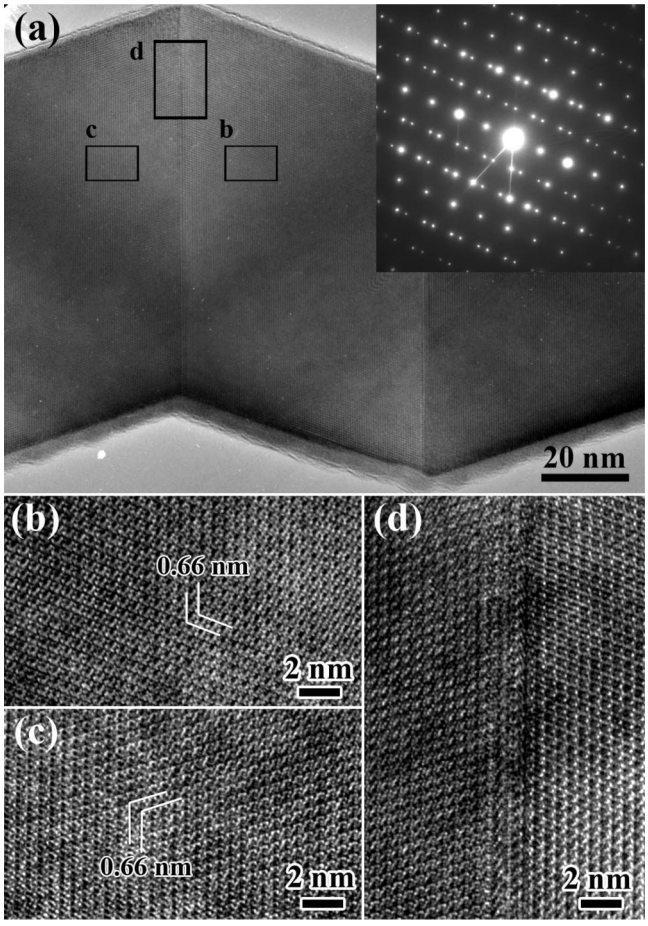

Figure 7. (a) TEM image and (b−d) HRTEM images of the twinned zigzag Zn_3P_2 nanowires.

kinks was observed, Figure 2e. Its SAED pattern is shown in the inset. This also reveals a single crystal. For the SAED patterns of both nanowire types the streaks were found along with the bright spots, indicating a high density of defects. In some cases, the nanowires are so curled that they form rectangle-shaped rings, as indicated in the bottom inset of Figure 2.

We studied the structures of the two Zn_3P_2 nanowire types using HRTEM, Figure 3a,b. TEM images and SAED patterns are consistent with the above discussions. The lower images are the HRTEM images taken in the vicinity of the kinks on each nanowire. The clearly observed lattice fringes are separated by 11.5 and 8.1 nm, in accord with the (001) and (100) interplane distances of a tetragonal Zn_3P_2, respectively. Thus we can deduce that the growth directions within the two kinks are the [001] and [101] orientations for the left-hand-side nanowire, and the [001] and [100] orientations for the right-hand-side nanowire. The presence of defects is in agreement with the SAED patterns.

For the synthesis of single-crystalline Zn_3P_2 nanowires, the source materials are ZnS and GaP powders and no catalysts were used. Besides, our characterizations show no particles attached to the wire tips, thus the growth of such nanowires is believed to be governed by the vapor−solid (VS) mechanism. ZnS reacted with graphite at high temperature via the reaction $ZnS\ (s) + C\ (s) \rightarrow Zn\ (g) + CS_2\ (g)$ to generate Zn vapors, which directly reacted with GaP vapors [$3Zn\ (g) + 2GaP\ (g) \rightarrow Zn_3P_2\ (g) + 2Ga\ (g)$] to form Zn_3P_2 vapors. The formed Zn_3P_2 vapors were transferred by the carrier gases to a low-temperature zone and deposited on the inner surface of the graphite crucible forming the final structures. The formation of zigzag, not straight nanowires suggested that the process is mainly controlled by the specific growth kinetics.[21−25] During the nucleation and growth processes, many factors should be considered, such as reaction temperatures, carrier gases, and a temperature increase speed.[21−25] All these parameters have influenced the final products, albeit the exact formation mechanism is uncovered at this stage of experiments.

3.2. Twinned Zigzag Zn_3P_2 Nanowires. With the introduction of In_2S_3 nanoparticles, another kind of zigzag Zn_3P_2 nanowires, the twinned wires, was obtained. Figure 4 depicts the XRD pattern of a sample. All peaks can be indexed to the tetragonal phase of a Zn_3P_2 crystal. Besides the peaks from the tetragonal phase of Zn_3P_2, a broad weak lump was found around 15−35°, indicating the presence of some amorphous products, which may be amorphous ZnO wrapped around the Zn_3P_2 nanowires (see the following discussion). No other sharp peaks were observed indicating the formation of pure Zn_3P_2 product.

Figure 5a is a SEM image of the product. Unexceptionally, the products also have zigzag shapes. Spherical particles were often found attached to the tips of the nanowires, indicating a vapor−liquid−solid (VLS) mechanism in the latter case, contrary to the VS-grown nanowires discussed above. On the other hand, microstructure studies found that the zigzag nanowires obtained in the presence of In_2S_3 have interesting periodic twins. Figure 5b shows a TEM image of two twinned nanowires. Periodic twins with a period of 50−120 nm along the nanowires are visible.

Panels a and b in Figures 6 show the TEM image of two other twinned nanowires. Spherical nanoparticles are attached to the wire tips (Figure 6c), again confirming the SEM result and verifying the VLS growth mechanism. The SAED pattern from two close twins is depicted in Figure 6d. Indexing of this pattern is presented in Figure 6e. The "twin" reflections are indexed with a subscript t and the remaining matrix reflections have no subscript. To obtain the composition information, we performed EDX on a single nanoparticle attached to a nanowire tip, the body of a nanowire, and its surface, Figure 6f−h. The nanoparticle is composed of In, the nanowire is made up of Zn and P, and the surface contains Zn and O, implying the existence of a thin layer of ZnO due to the surface oxidation by some residual oxygen in the synthetic chamber. In all these spectra the Cu signals originated from a copper TEM grid.

A high-magnification TEM image of a zigzag twinned Zn_3P_2 nanowire is depicted in Figure 7a. The corresponding SAED pattern is shown in the inset. Panels b−d of Figure 7 are the corresponding HRTEM images of the parts framed in panel a of Figure 7. The clearly resolved *d* spacings in all these images are 0.66 nm, corresponding to the (101) lattice distances of a tetragonal Zn_3P_2. According to Figure 7d, the twin boundaries are rich in defects, in line with the previous reports on twinned nanowires.[21−25]

The regarded VLS mechanism can be described as follows. In_2S_3 decomposes to generate In vapors at high temperature, which will be transferred to a low-temperature region and condenses in the form of In nanoparticles. These In nanoparticles act as catalysts for the growth of Zn_3P_2 nanowires. Due to the special experimental parameters, such as reaction temperatures, carrier gases, and temperature increase speed, twinned nanowires grow. During this process, In_2S_3 plays an important role. First, it decomposes to in situ generate metallic In catalysts for the nanowire growth. Second, both In and S vapors are simultaneously generated during the process, which affects the partial vapor pressure of the source materials and changes the growth kinetics. To confirm our suggestions, we substituted metallic

TABLE 1: A Bank of Produced Zn_3P_2 Nanostructures under Different Experimental Conditions

Zn_3P_2 products	experimental conditions: source	gases	temp/time	ref
nanotubes	ZnS:P:Mn_3P_2 3:1:1	N_2: 50 sccm (bottom)	1350 °C/1 h	6
trumpet-like nanowires	ZnS, GaP 0.5 g:0.35 g	N_2: 200 sccm (bottom)	1250 °C/1 h	7
nanobelts	ZnS:Mn_3P_2 1:1.2	Ar: 50 sccm (top), 250 sccm (bottom)	1350 °C/50 min	8
zigzag nanowires	ZnS:GaP 1:1.3	Ar: 150 sccm (bottom)	1400 °C/1 h	this work
	ZnS:GaP and In_2S_3 1:1.3	Ar: 150 sccm (bottom)	1400 °C/1 h	this work
nanowires	Zn_3P_2, ZnO, Zn 2:1:1	N_2: 25 sccm (laser ablation)	1100 °C/20 min	9

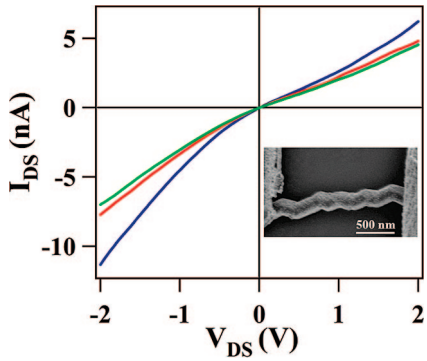

Figure 8. $I-V$ characteristics of a zigzag Zn_3P_2 nanowire device measured at different gate voltages (blue: Vg = −40 V; red: Vg = 0 V; and green: Vg = 40 V). Inset: SEM image of a typical zigzag Zn_3P_2 nanowire device.

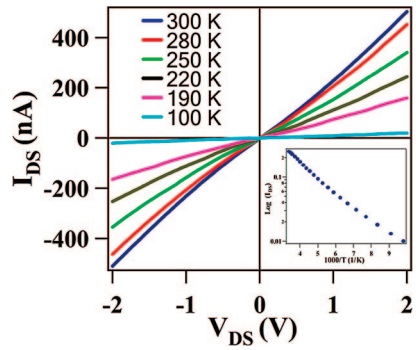

Figure 9. Temperature-dependent $I-V$ characteristics of a zigzag Zn_3P_2 nanowire device. Inset: The conductance of the device in a logarithmic scale at zero bias voltage plotted as a function of 1000/T.

In particles for In_2S_3. However, no twinned nanowires were found in the latter case and the products consisted of some straight nanowires with many big particles.

Previously, different kinds of 1-D Zn_3P_2 nanostructures, nanotubes, trumpet-like nanowires, and nanobelts, were produced using a thermochemical method by the present authors and using a laser-ablation method by Wang et al., as listed in Table 1.[6−9] At first glance, it seems that those products were produced at very similar conditions. However, a deeper analysis shows that this is not true. As is well-known, the structures, compositions, and morphologies of the products during a vapor phase growth are greatly influenced by the experimental parameters, such as source materials, flowing gases, pressures, source temperature, substrate temperatures, catalysts, etc. A slight change in any parameter results in quite different products.[26−29] For example, ZnO nanobelts were produced by using a ZnO powder as the source material at 300 Torr.[26] However, while introducing In_2O_3 and lithium carbonate into the system, seamless ZnO nanorings were produced instead of nanobelts.[27] Another kind of ZnO nanostructure, superlattice ZnO nanosprings, was produced instead of nanobelts with the only change being the system pressure.[28] Many other reports have also confirmed a prime influence of marginal experimental parameter changes on the final products. For example, Zn_3P_2 nanotubes were produced by using ZnS, P, and Mn_3P_2 as the source materials under a 50 sccm (bottom) N_2 gas flow. Zn_3P_2 nanobelts were produced by using ZnS and Mn_3P_2 as the source materials under 50 sccm (top) and 250 sccm (bottom) Ar gas flows. By contrast, zigzag nanowires were produced in the present work; however, the details still need to be clarified.

3.3. Electrical Transport Properties. The inset in Figure 8 shows a SEM image of a typical device with a channel width of about 1.5 μm, where a zigzag nanowire can be seen bridging two Ti/Au electrodes. It also illustrates its $I-V$ curves measured at room temperature and at different gate voltages. The curves exhibit a linear response, indicating that Ohmic contacts were achieved between the metal electrodes and nanowires. For a given source-drain voltage, current increases with an increase in gate voltage, indicating that the zigzag Zn_3P_2 nanowires are of the p-type. The gate effect is rather weak, which is probably due to the high density of defect sites within the nanowires.

Then the $I-V$ characteristics of the device were studied at different temperatures, Figure 9. A progressive reduction of the device conductance was observed as the temperature decreased. The zero-bias conductance was calculated to be 205.75 nano-Siemens (nS) at 300 K, while it decreased to 17.38 nS at 100 K. The conductance of the device in a logarithmic scale at zero bias voltage is plotted as a function of 1000/T, the inset to Figure 9. Within the temperature region studied, the conductance versus temperature can be fitted into the formula $G \approx \exp(-E_\alpha/K_BT)$, with E_α = 49.7 meV, suggesting the thermal activation of carriers to be the dominant transport mechanism.[11]

4. Conclusion

In summary, single-crystalline and twinned zigzag Zn_3P_2 nanowires have successfully been synthesized via a simple thermochemical process. Two kinds of *single-crystalline* zigzag nanowires were found to coexist in the products: the wires display the angles between every two neighboring kinks either of 120° or 90°. In addition, *twinned* zigzag nanowires were produced via a vapor−liquid−solid process in the presence of catalysts. Prototype devices based on individual zigzag nanowires were fabricated and studied. The studies reveal that the zigzag Zn_3P_2 nanowires are p-type semiconductors and the thermal activation with an energy of 49.7 meV is the dominant transport mechanism.

Acknowledgment. The authors acknowledge financial support from the L. K. Whittier Foundation and the National Science Foundation (CCF-0726815 and CCF-0702204).

References and Notes

(1) Bhushan, M.; Catalano, A. *Appl. Phys. Lett.* **1981**, *38*, 39.
(2) Fessenden, R. W.; Sobhanadri, J.; Subramanian, V. *Thin Solid Films* **1995**, *266*, 176.
(3) Bhushan, M. *Appl. Phys. Lett.* **1982**, *40*, 51.

(4) Bichat, M. P.; Pascal, J. L.; Gillot, F.; Favier, F. *Chem. Mater.* **2005**, *17*, 6761.
(5) Kishore, M. V. V. M. S.; Varadaraju, U. V. *J. Power Sources* **2005**, *144*, 204.
(6) Shen, G. Z.; Bando, Y.; Ye, C. H.; Yuan, X. L.; Sekiguchi, T.; Golberg, D. *Angew. Chem., Int. Ed.* **2006**, *45*, 7568.
(7) Shen, G. Z.; Bando, Y.; Hu, J. Q.; Golberg, D. *Appl. Phys. Lett.* **2006**, *88*, 143105.
(8) Shen, G. Z.; Bando, Y.; Golberg, D. *J. Phys. Chem. C* **2007**, *111*, 5044.
(9) Yang, R. S.; Chueh, Y. L.; Morber, J. R.; Snyder, R.; Chou, L. J.; Wang, Z. L. *Nano Lett.* **2007**, *7*, 269.
(10) Shen, G. Z.; Ye, C. H.; Golberg, D.; Hu, J. Q.; Bando, Y. *Appl. Phys. Lett.* **2007**, *90*, 073115.
(11) Liu, X.; Li, C.; Han, S.; Han, J.; Zhou, C. *Appl. Phys. Lett.* **2003**, *82*, 1950.
(12) Liu, Z.; Zhang, D.; Han, S.; Li, C.; Tang, T.; Jin, W.; Liu, X.; Lei, B.; Zhou, C. *Adv. Mater.* **2003**, *15*, 1754.
(13) Li, C.; Zhang, D.; Han, S.; Liu, X.; Tang, T.; Zhou, C. *Adv. Mater.* **2003**, *15*, 143.
(14) Gates, B.; Wu, Y.; Yin, Y.; Yang, P. D.; Xia, Y. N. *J. Am. Chem. Soc.* **2001**, *123*, 11500.
(15) Law, M.; Goldberger, J.; Yang, P. D. *Annu. Rev. Mater. Res.* **2004**, *34*, 83.
(16) Dai, Z. R.; Pan, Z. W.; Wang, Z. L. *Adv. Funct. Mater.* **2003**, *13*, 9.
(17) Duan, X. F.; Lieber, C. M. *Adv. Mater.* **2000**, *12*, 298.
(18) Cui, Y.; Zhong, Z. H.; Wang, D. L.; Wang, W.; Lieber, C. M. *Nano Lett.* **2003**, *3*, 149.
(19) Wang, D. W.; Dai, H. J. *Angew. Chem., Int. Ed.* **2002**, *41*, 4783.
(20) Zhu, J.; Peng, H.; Chan, C. K.; Jarausch, K.; Zhang, X. F.; Cui, Y. *Nano Lett.* **2007**, *7*, 1095.
(21) Zhou, X. T.; Sham, T. K.; Shan, Y. Y.; Duan, X. F.; Lee, S. T.; Rosenberg, R. A. *J. Appl. Phys.* **2005**, *97*, 104315.
(22) Zhan, J.; Bando, Y.; Hu, J.; Xu, F.; Golberg, D. *Small* **2005**, *1*, 883.
(23) Fang, X. S.; Ye, C.; Zhang, L.; Xie, T. *Adv. Mater.* **2005**, *17*, 1661.
(24) Shen, G. Z.; Bando, Y.; Liu, B.; Tang, C.; Golberg, D. *J. Phys. Chem. B* **2006**, *110*, 20129.
(25) Duan, J.; Yang, S.; Liu, H.; Gong, J.; Huang, H.; Zhao, X.; Zhang, R.; Du, Y. *J. Am. Chem. Soc.* **2005**, *127*, 6180.
(26) Pan, Z. W.; Dai, Z. R.; Wang, Z. L. *Science* **2001**, *291*, 1947.
(27) Kong, X. Y.; Ding, Y.; Yang, R. S.; Wang, Z. L. *Science* **2004**, *303*, 1348.
(28) Gao, P. X.; Ding, Y.; Mai, W.; Hughes, W. L.; Lao, C.; Wang, Z. L. *Science* **2005**, *309*, 1700.
(29) Dai, Z. R.; Pan, Z. W.; Wang, Z. L. *Adv. Funct. Mater.* **2003**, *13*, 9.

JP806334K